ELSEVIER

Airborne Digital Camera Image Semivariance for Evaluation of Forest Structural Damage at an Acid Mine Site

*Josée Lévesque** *and Douglas J. King*†

A forest downstream of a heavy metal acid tailings area at the KamKotia mine site near Timmins, Ontario shows visible signs of damage which include varied leaf size, leaf discoloration, dead branches, and increased individual tree crown and forest canopy openness. High resolution remote sensing has potential for providing means to spatially and temporally evaluate such damage. In particular, image texture can be used in modeling forest and individual tree structural variations which may result from stress. In this study, an airborne multispectral digital camera system was used to acquire imagery with ground pixel spacing of 0.25 m, 0.5 m, and 1.0 m. Relations of image semivariance measures with field forest structure and health measures were determined. Semivariograms were derived using two sampling techniques: transects in two perpendicular directions, and omnidirectional sampling within pixel matrices. Sampling was conducted over the forest canopy as well as within individual tree crowns. The principal objective of the study was to determine the types of forest canopy and individual tree crown structure and health information captured by semivariograms at the three spatial resolutions. In canopy scale sampling, the 1 m pixel semivariograms were best related to forest canopy closure, stem density, and a visually derived tree stress index. The 0.5 m pixel semivariograms related better to tree crown size and tree height. The transect technique was more sensitive to tree height and the matrix technique produced stronger relations with tree stress. In individual tree crown samples, the 0.25 m pixel semivariograms were well related to tree crown closure. This suggests that semivariograms extracted from the 1 m and 0.5 m pixel images are suitable for mapping structural and textural information related to forest damage at the canopy level while the semivariograms extracted from the 0.25 m pixel images depict information at the tree crown level. ©Elsevier Science Inc., 1999

INTRODUCTION

The environmental impact of acid mine drainage on surrounding forested areas is a growing concern for many mine operators and government agencies. Complex chemical weathering reactions, initiated when sulfide waste rock and tailings are exposed to oxygen and water, lead to the production of sulfuric acid (Kelley and Tuovinien, 1988). Acidic drainage may wash soil nutrients away reducing their availability to vegetation. It also causes the release into the soil of toxic substances, such as heavy metals and other substances related to mine exploitation, which can interfere with plant nutrient uptake and growth. Symptoms of tree damage can be expressed in various physiological and morphological changes such as early senescence, chlorosis, stunted or oversized growth, and loss of foliage. Forest canopy damage may be evident as reductions in structural variables such as stem density, canopy closure, or other variables related to vegetation production. These stress and damage characteristics may be manifested as spectral and textural characteristics in remotely sensed images at both the individual tree crown and forest canopy scales (Murtha, 1978; Curtiss and Maecher, 1991).

Several authors have used image semivariograms to extract forest damage and structural information. For ex-

* Ottawa-Carleton Geoscience Centre, Department of Earth Science, Carleton University, Ottawa, Ontario, Canada

† Department of Geography, Carleton University, Ottawa, Ontario, Canada

Address correspondence to J. Lévesque, Canada Centre for Remote Sensing, 588 Booth St., Ottawa, ON K1A 0Y7, Canada. E-mail: levesque@ccrs.nrcan.gc.ca

Received 13 December 1997; revised 26 October 1998.

REMOTE SENS. ENVIRON. 68:112–124 (1999)

655 Avenue of the Americas, New York, NY 10010

0034-4257/99/$–see front matter
PII S0034-4257(98)00104-7

ample, Bowers et al. (1994) used semivariance statistics (range, sill, nugget) derived from SPOT HRV panchromatic and multispectral data to separate and model Balsam fir (*Abies balsamifera*) damage caused by the woolly adelgid. Cohen and Spies (1990) used semivariograms of 1 m, 10 m, and 30 m resolution airborne video images to extract structural and textural information for Douglas-fir (*Pseudotsuga menziesii*) canopies. Wulder et al. (1997) introduced the Semivariance Moment Texture measure, derived from the semivariogram statistics of 1 m resolution *casi* (Compact Airborne Spectrographic Imager) images, as a textural indicator which is related to canopy leaf area index (LAI) for both homogenous and heterogeneous cover types. In a study to predict tree height, tree crown diameter, and canopy density, St-Onge and Cavayas (1995) used the directional variogram approach with MEIS II (Multi-detector Electro-optical Imaging Scanner) images having spatial resolutions ranging from 0.36 m to 2.16 m. Coops and Catling (1997) plotted the mean values of the standard deviation at increasing window size to extract local variance in a 2 m pixel video image in an attempt to characterize the complexity of habitat in forest environments at different spatial resolutions. A common element of multiresolution studies is that higher resolution imagery typically provides better relations with forest structural variables. In this research, this knowledge is extended to analysis of individual tree crown structure as well as forest structure using imagery of less than, or equal to, 1 m pixel spacing.

The abandoned KamKotia mine site near Timmins, Ontario, is undergoing a serious acid drainage problem and is a continuous source of heavy metal pollutant stress in the surrounding forest environment. This article evaluates the relationships between high resolution image semivariance (as a measure of texture) and forest structural characteristics and tree health conditions at the KamKotia site. It is part of a research program in which the goal is to develop integrated image spectral, textural, and structural models for mapping of the dynamics of forest health in ecosystems subjected to such localized stress (King, 1995a).

Research Objective

The principal objective of this research was to determine whether semivariogram statistics from high resolution imagery can be used to model subtle structural variations within the forest canopy and within individual tree crowns that are related to various degrees of damage. More specifically, images with pixel spacing of 0.25 m, 0.5 m, and 1 m were analyzed to determine the spatial resolution required to extract such information at both the forest canopy and individual tree crown levels. Semivariogram range, sill, and nugget were derived from airborne digital camera images using the matrix and transect techniques of Cohen and Spies (1990). The semivariogram statistics were used in correlation analysis to determine the strength of relationships with forest canopy and tree crown measures.

METHODOLOGY

Study Site Establishment

The KamKotia zinc and copper deposit was mined for about 20 years, ceasing operation in the early 1970s. It was selected as the study location because of its known acid drainage problems and its fairly simple physiography. Three large tailings areas totaling about 350 ha surround the original mine to the north, northeast, and south. A 7 m high dam impounds the north tailings, but it is leaking into the northeast tailings which is not contained in any way. Surface drainage from the northeast unimpounded tailings follows two creeks, which exit the tailings from its northern boundary (see Fig. 1a). The pH of water in these creeks was measured at between 1.4 and 2.0 in August of 1993 and 1994. The creeks are approximately 1.2 km apart. Although both flow in a northerly direction, the western creek bends around to the east after about 400 m and flows towards the eastern creek, which it joins to form a single northerly flowing creek. The two creeks effectively delimit an area of forest about 1.2 km long (east–west) by 400 m on the west side to 680 m on the east side. While surface drainage follows the creeks around this forested area, analysis of the 1:10,000 Ontario Ministry of Natural Resources Base map for the site revealed a gentle topographic slope from the tailings edge to the northern boundary of the forest area, with an average slope of about 1°. It was therefore hypothesized that metal contaminated near-surface groundwater originating in the tailings would flow in a near northerly direction through the forested area perpendicular to the contour lines. Thus, a study area was selected between the two creeks (Fig. 1a), and six plots were established along an 800 m transect starting from the mine tailings and following the drainage direction (Fig. 1b). Plots 1–3 are 100 m apart and the others are between 150 m and 200 m apart. The furthest plot from the mine tailings, plot C (control), was used as a reference as it is located on slightly higher ground across the west/north creek and should not be affected by the acidic drainage. Each plot covers an area of 50 m×50 m.

The soils vary along the transect from predominantly sandy to more loamy but with no known spatial trend. The forest is composed of mature trembling aspen (*Populus tremuloides*) with a mean age of 76 years (s=12.9, n=30), a few small pockets of codominant balsam poplar (*Populus balsamifera*), and an understory of young black spruce (*Picea mariana*), white spruce (*Picea glauca*), and balsam fir. The transect was deliberately located within this aspen stand because of: i) the known sensitivity of aspen to airborne pollutants such as SO_2 and heavy metal

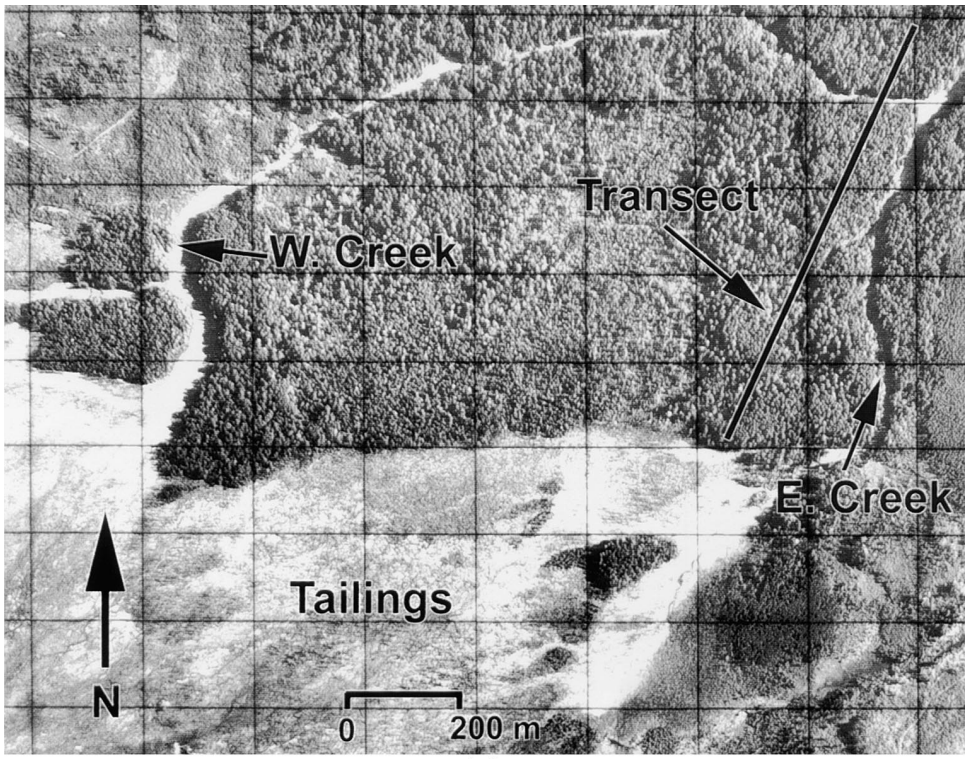

(a)

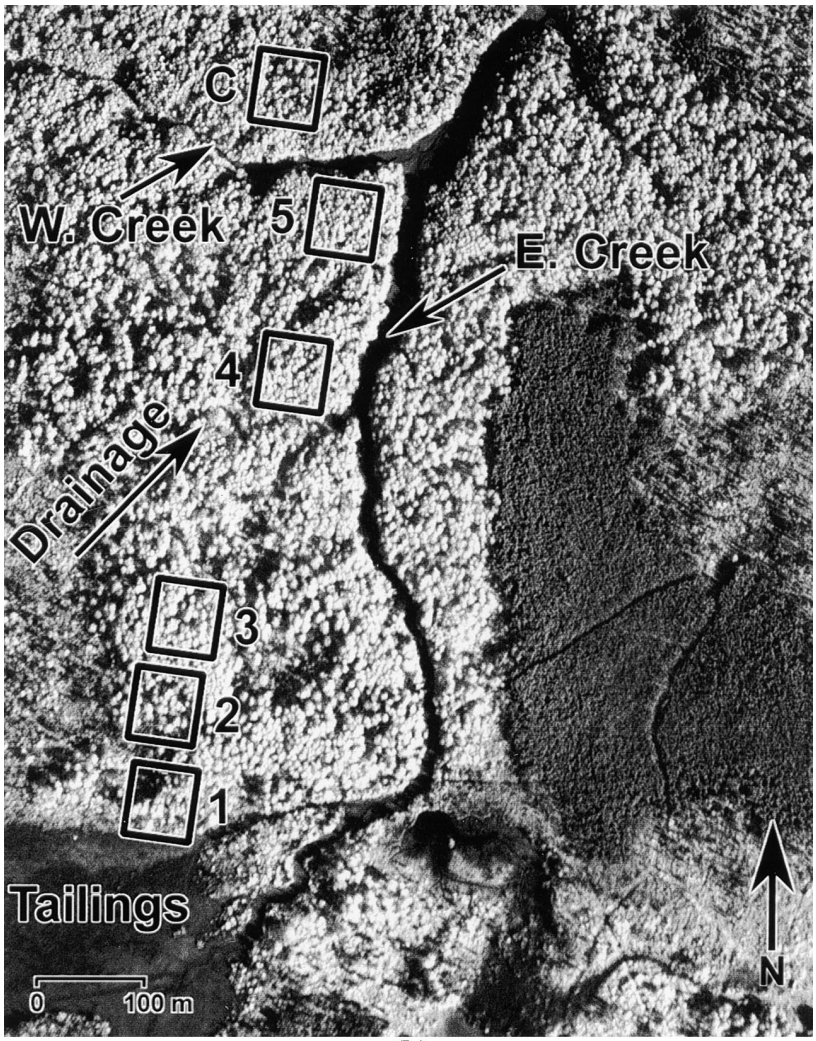

(b)

Figure 1. KamKotia mine site study area: (a) scanned 1991 air photo (showing georeferenced grid) of the northern section of the mine site, pixel spacing=0.5 m, and (b) near-infrared digital camera image of study site, 7 September 1995. Pixel spacing is 1 m.

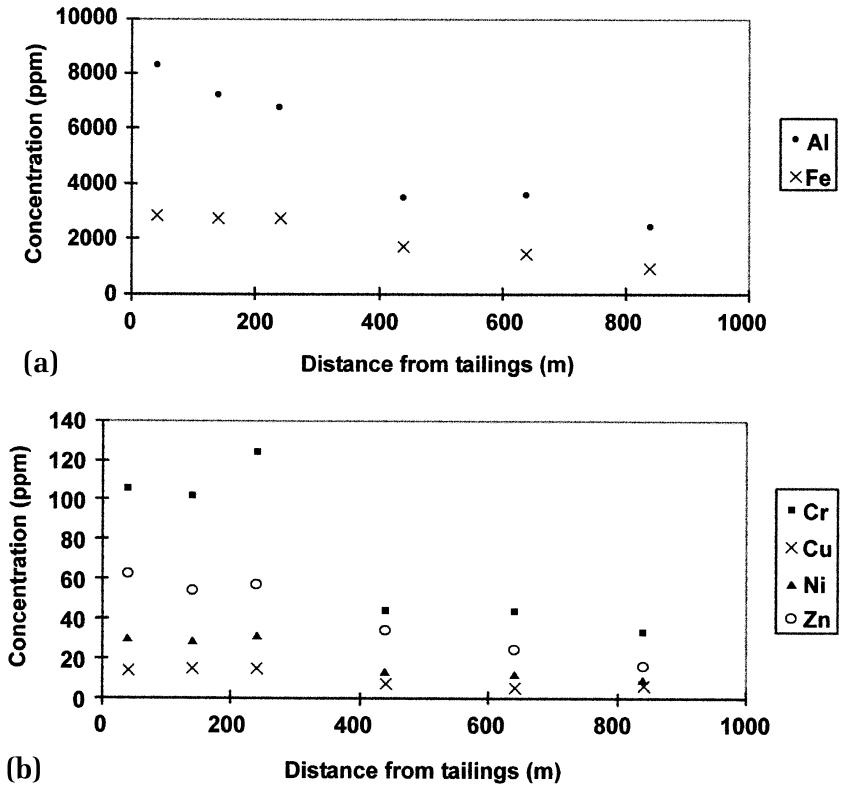

Figure 2. Concentration of a) aluminum and iron (ppm) and b) chromium, copper, nickel, and zinc (ppm) in the soil B horizon, August 1993 versus distance from the tailings edge (m)

emissions, which is analogous to windblown deposition of pollutants from the high sulfur tailings, ii) aspen's preference for alkaline soils making it less tolerant to acidic environments than other boreal forest species (Peterson and Peterson, 1992), and iii) the high potential for mechanical effects of wind from the tailings to exacerbate the gradual deterioration of this mature stand.

Field Data Acquisition and Analysis

Soil Chemistry

To determine if soil metal concentrations vary along the transect, soil samples from each of the A, B, and C horizons were collected at five random locations along the axis perpendicular to the apparent drainage direction up to a distance of 25 m from the center of each plot. This soil sampling was conducted in May and August of 1992 and 1993 and August of 1994 and 1995. Chemical analyses using ICPES (Inductively Coupled Plasma Emission Spectrometry) techniques were conducted to determine concentrations of 9 metals (Al, Cr, Cu, Fe, Mn, Ni, Pb, Ti, and Zn) in soil solutions extracted using aqua regia digestion. Initial results from the 1992 data were presented in Lévesque and King (1993).

Figure 2a shows example concentrations of aluminum and iron in parts per million at each plot from the August 1993 data. Figure 2b shows example concentrations of chromium, copper, nickel, and zinc in parts per million from the same August 1993 data. These data are means of the five values in the B horizon (where the tree root zone is mostly located). The variation in each element's measured concentration (from the five samples at each plot) was quite high and did not consistently result in statistically significant changes in concentration between any plots on the transect. However, the data do indicate a trend of decreasing metal concentration with distance from the tailings, particularly after 200–400 m. The control plot typically had the lowest concentrations.

The same trend was present for all other elements, for all horizons, and for all sample dates. It was not the objective of this study to determine if such metal concentrations, in combination with measured soil pH between 4.2 and 6.8 at the plots, were causal factors of the observed forest damage. The relatively high levels of aluminum and iron near the tailings may contribute to forest damage, but the concentrations of the other elements may not be toxic. Instead, this observed trend in soil chemistry was used to verify that the transect was well positioned and to partially justify continued development of the field and airborne experimental design.

Forest and Individual Tree Structure and Stress Measurements

A total of 180 dominant and codominant trees, 30 in each plot, which would be visible to the sensor were measured to derive six forest canopy and tree crown variables. The following six variables describe the structural and health characteristics of each of the plots and were used to quantitatively relate images to field data: 1) Forest canopy closure was measured visually from the

ground in 5% increments with the aid of a calibrated chart showing the proportion of a black surface on white background. Evaluation of three repetitions on different days for a sample of 15 trees in the first and last plots of the transect produced an average standard deviation of 4.3% which is less than the measurement increment. For comparison, in later analysis, measurements made using this visual technique were found to be highly correlated with LICOR LAI-2000 canopy closure measurements for the same plots (r=0.87) (Li-CoR Inc., 1990). 2) Forest stem density was measured as the number of trees per 10 m×10 m area. 3) Tree crown size was determined from the average of two measurements using a measuring tape along the major and minor axes projected to the ground. 4) Tree height was measured using an hypsometer. 5) Individual tree crown closure was measured using the same calibrated chart that was used for canopy closure. Similar repetitions of three measurements resulted in an average standard deviation of 3.51%, which is less than the measurement increment. 6) A tree stress index was devised and measured in increments of 0.5 between 1 (healthy) and 5 (dead) and was assessed by viewing each tree crown from the ground from several angles. Emphasis was placed on the visual symptoms that would be manifested as image spectral or textural variations. The characteristics were adapted from a deciduous tree decline index developed by the Ontario Ministry of Environment (McIlveen et al., 1989) and utilized in research on remote sensing of sugar maple (*Acer saccharum*) decline by the coauthor (in Yuan et al., 1991). Each sampled tree was systematically evaluated for: crown morphology (asymmetric, circular, thin), foliage density (dense, medium dense, sparse, clustered), foliage size (undersized, full size), foliage color (deep green, light green, discolored), proportion and location of dead branches, amount and type of trunk defects (cankers, cracks, moss, fungus, etc.), and tree lean, including the proportion of each leaning tree which was dying and the proportion dead. To test the precision of these health measurements, 30 trees were randomly selected and assessed by a second observer three times over a period of 6 weeks. The average of the standard deviations derived from these health measures was 0.238, which indicates good precision for this visually-based index.

Two scales of analysis were conducted using the above data: 1) At the canopy scale, determination of relations of forest canopy and individual tree measurements averaged over each plot with plot image texture, and 2) at the tree scale, determination of individual tree crown closure with image texture measured within tree crowns. The distinction between forest canopy closure (variable 1 above) and individual tree crown closure (variable 5 above) as defined in this article is critical to the two-scale analysis of this study.

Imagery Acquisition

A digital camera sensor incorporating a Kodak Megaplus 1.4 black and white, 1320×1035 pixel format camera was used. The camera is entirely computer controlled, with a rotating filter wheel providing 8-bit data in up to eight spectral bands between 430 nm and 1000 nm (King, 1995a,b). It can be mounted in small single or twin engine aircraft which has been modified for vertical aerial imaging. The view angle of the camera is ±9.1×7.2 degrees using a 28 mm focal length lens. Such a small view angle was used in this research to minimize spatial nonuniformity of response from optical, BRDF, and atmospheric effects (these effects are currently being analyzed in a separate research project using larger angles of view). Imagery was acquired on 23 August 1993 with 0.5 m and 1.0 m ground pixel spacing. The spectral bands were: blue (430–470 nm), green (545–555 nm), red (665–675 nm), and near-infrared (795–805 nm) corresponding to the major vegetation spectral absorption and reflectance regions in the visible and near-IR. After initial analysis of this imagery it was determined that sampling and analysis within individual tree crowns would only be possible using imagery with a smaller pixel spacing since the semivariance range was not reached in 70% of the cases when using the 0.5 m resolution images. Consequently, a second set of imagery using the same spectral bands was acquired on 7 September 1995 (just before autumn leaf color change) with 0.25 m and 0.5 m pixels. The second set of 0.5 m pixel imagery was acquired for comparison of individual tree crown sampling with the forest canopy-based sampling of the 1993, 0.5 m pixel imagery. The near-IR band was selected for analysis, as this band had the best exposure and contrast in both data sets.

Image Analysis: Semivariogram Calculation

Semivariance S^2 is half of the squared difference between pixel digital numbers z, at two locations, x and $x+h$ (after Curran, 1988) (Eq. 1):

$$S^2=\tfrac{1}{2}[z(x_i)-z(x_i+h)]^2. \quad (1)$$

The semivariogram $Y(h)$ is a graphical representation of the average semivariance of several pixel pairs at each lag (h). It displays the spatial variability within the data set (Cohen and Spies, 1990) by capturing the variance between spatially separated pixels (Wulder et al., 1997). The semivariogram is calculated in Eq. (2) as (Curran, 1988)

$$Y(h)=\frac{1}{2m}\sum_{i=1}^{m}[z(x_i)-z(x_i+h)]^2, \quad (2)$$

where m is the number of pairs of pixels separated by the same lag. Thus, $Y(h)$ is obtained for each lag and plotted against lag. Mathematical models are fit to a semivariogram by least squares techniques to determine

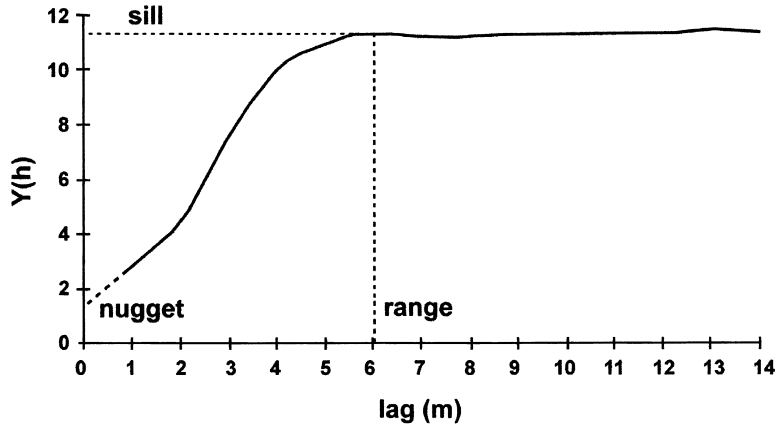

Figure 3. Example of a spherical shape semivariogram showing the sill, the range and the nugget.

the range, the sill, and the nugget. Figure 3 shows an example of a spherical shape semivariogram with the range, the sill, and the nugget. In this model, the pixels at small lags are more likely to have lower semivariance than at greater lags, with semivariance increasing until a maximum is reached at the *sill.* The lag at which this maximum is reached is called the *range* and is interpreted as a measure of spatial dependence of the data. The range is often associated with the size of individual objects such as tree crown size in high resolution imagery or forest stand size in low resolution imagery (Woodcock, 1988a, b). The *nugget* is an estimate of the variability at a lag of zero and is essentially a function of support size relative to object size.

The shape of the semivariogram provides information about the structure of an image scene. The spherical shape semivariogram is typical of an image where pixels become completely independent above the range. In contrast, the periodic shape semivariogram shows a repetitive pattern where the semivariance of pixels further apart is less than pixels closer to each other (e.g., rows in cultivated lands). The linear semivariogram increases constantly and does not reach the range. It often occurs when the distance used is not great enough to reach the maximum variability between pixels.

In this research, sample pixel matrices and transects were extracted from the imagery and used to calculate omnidirectional and directional semivariograms, respectively. Pixel matrices were extracted over areas of 30×30 pixels. Omnidirectional semivariograms, calculated from these matrices, were derived using multiple lags from all possible directions within a 90° angle as shown in Figures 4a,b. Where more than one matrix was sampled for a given plot, the average range and sill of the resulting omnidirectional semivariograms were calculated. For the transect method, three lines of 50–100 pixels were sampled in perpendicular directions (the image horizontal and vertical) as shown in Figure 4c. An average range and sill was calculated from the six individual semivariograms. Calculations for initial analyses were made using the program GEOEAS (Englund and Sparks, 1991) while later analyses were conducted using VARIOWIN which was easier to implement (Pannatier, 1994). Analysis was conducted at the forest canopy scale using the 1993, 0.5 m and 1 m pixel data, and at the individual tree crown scale using the 1995 0.25 m and 0.5 m pixel data. The nugget, range, sill, and shape of the semivariogram were determined from the fitted spherical models. The indicative goodness of fit (Pannatier, 1994) ranged from 0.003959 to 0.0138 for all semivariograms. These small deviations from a perfect goodness of fit of zero indicate that very little error in the semivariogram parameters was introduced by the spherical function fit to the semivariance data. The range and sill were then linearly correlated with the forest and tree measures for analysis of the strength of the relationships between the image and field variables. In some cases, the semivariogram displayed linearity, which meant that the range was not reached.

Forest Canopy-Scale Sampling

In canopy-scale sampling for semivariance analysis, pixel matrices and transects were placed over many trees and gaps in each plot. Figures 4a,b illustrate pixel matrix extraction for the canopy-scale analysis. For the 0.5 m pixel image (Fig. 4a) nine matrices of 30×30 pixels (15 m×15 m) each were extracted at each plot. The whole plot area was not used as a matrix because by splitting the plots into subplots, it was possible to observe the within-plot variation. A good example of the within-plot variation is noticeable in plot 1 where almost one quarter of its surface in the NW part is an open area (Fig. 1b). The number of trees sampled in these quadrants ranged from 12 to 41. For the 1 m pixel image (Fig. 4b) only 4 matrices of 30×30 pixels (30 m×30 m) needed to be extracted in order to cover the whole plot area.

Figure 4c shows schematically the use of transects for sampling at the canopy scale in both the 1 m and 0.5 m pixel images. A total of six transects, three in the E–W direction and three in the N–S direction, were extracted from each plot, each covering a minimum of

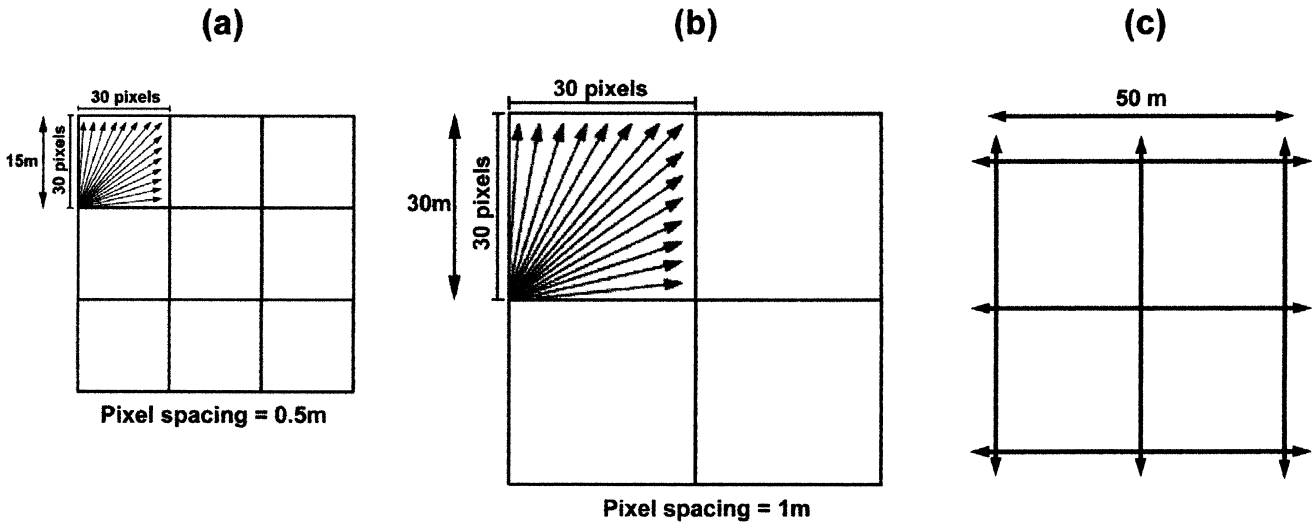

Figure 4. Illustration of canopy-scale semivariance sampling techniques: a) the matrix technique with omnidirectional sampling for the 0.5 m pixel image, b) the matrix technique with omnidirectional sampling for the 1 m pixel image, and c) the transect technique with sampling in two directions for both the 0.5 m and 1 m pixel images.

eight trees. To cover the 2500 m^2 area of the plots, the transects were 25 pixels (25 m) apart in the 1 m pixel image and 50 pixels (25 m) apart in the 0.5 m pixel image. The transects have a length of 50 pixels (50 m) in the 1 m pixel image and 100 pixels (50 m) in the 0.5 m pixel image.

Individual Tree Crown-Scale Sampling

In sampling of individual trees, only the matrix technique was used. The transect technique was not used because any transect within a single tree crown contained too few pixels to reach the range. For the matrix technique, many more points are accumulated and statistically valid sampling could be achieved for most trees at each plot. In the 0.25 m pixel imagery, the support size (pixel) was between 1/20 and 1/32 the object (tree) widths and twice that in the 0.5 m pixel imagery. Pixel matrices were extracted from 30 and 20 tree crowns in the 1995 0.25 m and 0.5 m pixel images, respectively. The sampled trees are the same in both images and are divided approximately equally in numbers between all plots. It was not possible to sample 10 of the trees at the 0.5 m resolution because their crowns were too small, leaving too few pixels to extract for the semivariance analysis. The matrix sizes varied between 10 by 10 pixels and 21 by 21 pixels depending on tree crown size and image pixel spacing.

RESULTS AND DISCUSSION

Forest Canopy and Individual Tree Crown Measurements

Table 1 lists the mean (avg) and standard deviation (std) of the forest canopy and tree crown measurements at each plot. For any given variable there are several pairs of plots with significantly different mean values at the 0.05 level. In many of the significantly different plot pairs, one is from the first three plots (40–240 m from the tailings) while the other is from the last three plots (440–840 m from the tailings).

Thus, the most evident spatial trend in the data is the clustering of plots near the tailings (e.g., plots 1, 2, and perhaps 3), and plots further from the tailings (e.g., 4, 5, 6) for all measurements except individual tree crown closure. The first three plots have consistently larger crown size, taller trees, lower stem density, lower canopy closure (except for plot 3), and higher stress index than the last three plots. The fact that the plots closer to the mine tailings have larger crown size and taller trees does not mean they are healthier than plots further from the tailings. In fact, a larger number of standing and fallen dead trees are present in these three plots compared to the last three as expressed by their lower canopy closure and stem density. It suggests that the remaining large trees have thus far been able to withstand the chemical and mechanical stresses and they may have experienced greater growth rates because of the thinning of the forest. Consequently, of the variables evaluated, the stress index, forest canopy closure, and stem density most directly reflect the higher structural damage in the first three plots.

These results are supported by a temporal analysis of the site conducted by Walsworth and King (1997). They evaluated individual tree death and regrowth for the period 1946–1991 using neighborhood-based transition analysis of digitized aerial photography. A statistically significant decrease in stem density in the area of the first three plots of this study was found to have occurred during the period from initial deposition of the unimpounded tailings to 1991 with the forest tending towards greater heterogeneity. In addition, results from a 1997 field study of 55 plots in the area between the two creeks

Table 1. Average (avg) and Standard Deviation (std) of Forest Canopy and Tree Measures for Each Plot

		Plot					
		1	*2*	*3*	*4*	*5*	*C (Control)*
Forest canopy closure (%)	avg	40.83	40.00	56.67	50.00	66.67	55.00
	std	25.23	16.90	11.06	17.89	9.43	18.71
Forest stem density	avg	7.33	5.50	5.60	9.20	18.25	16.43
(per 100 m^2)	std	1.89	2.14	2.80	1.83	3.90	6.84
Tree crown size (m)	avg	6.42	7.79	8.14	5.54	5.43	6.38
	std	1.37	1.86	1.93	1.49	1.24	2.25
Tree height (m)	avg	26.88	26.60	30.32	24.58	24.93	25.67
	std	1.90	2.68	3.37	3.04	3.27	6.12
Tree crown closure (%)	avg	62.30	67.00	62.40	72.30	63.70	59.00
	std	10.90	10.70	11.80	9.37	16.70	13.40
Tree stress index	avg	2.77	2.66	2.58	2.53	2.37	2.53
(1=healthy to 5=dead)	std	0.62	0.75	0.70	0.59	0.82	0.67

(Fig. 1a) (Olthof, 1997) have shown statistically significant decreases in leaf area index and the number of fallen trees as well as a significant increase in stem density with increasing distance from the tailings. These results help to confirm and quantify the spatiotemporal variation in forest structure that is evident when the site is visited over several years.

Forest Canopy-Scale Image Semivariance Analysis

Table 2 shows the correlation coefficients and associated significance levels of the relationships between the ground-based measurements and the semivariogram range and sill for the 1993 1 m and 0.5 m images derived from both the transect and matrix techniques by sampling over the forest canopy. Correlation coefficients greater than, or equal to, 0.811 are significant at the 0.05 level or better and are underlined.

Relations with Forest Canopy Measurements

Of the forest canopy variables, both the range of the 1 m pixel transect and matrix semivariograms are positively well correlated with forest canopy closure. Figure 5a shows this relationship for the 1 m pixel transect semivariogram. The range increases with canopy closure in this mature boreal forest since the tree crowns are closer to each other, and they produce a more homogeneous gray tone surface in the imagery. Such a relation would not apply in sparse forest conditions unless the spatial variability of the understory and other surface cover was high for the given pixel spacing. Figure 5b shows the relation between the range of the 1 m pixel matrix semivariogram and stem density per 100 m^2. As for canopy closure, as stem density increases, a more homogeneous gray tone surface is produced and the range increases. Transect semivariograms are not highly correlated with this forest measurement possibly because they represent sparser samples than do the matrices.

Relations with Individual Tree Measurements

Of the individual tree variables, tree crown size is well correlated with the range values of both the 0.5 m pixel transect and matrix semivariograms extracted over the canopy. Figure 6a shows the graphical representation of the relationship between range and tree crown size for

Table 2. Correlation Coefficients (r) between the Field Forest Canopy and Tree Measurements and the Semivariogram Parameters for the Matrix and Transect Techniques

	Transect				*Matrix*			
	Range 0.5 m	*Sill 0.5 m*	*Range 1 m*	*Sill 1 m*	*Range 0.5 m*	*Sill 0.5 m*	*Range 1 m*	*Sill 1 m*
Forest canopy closure (%)	−0.16	0.28	0.92	0.36	−0.32	−0.70	0.83	−0.15
	p=.724	p=.549	p=.003	p=.433	p=.489	p=.081	p=.025	p=.748
Forest stem density	−0.60	−0.38	0.44	−0.26	−0.70	−0.54	0.81	−0.15
(per 100 m^2)	p=.154	p=.404	p=.321	p=.578	p=.081	p=.215	p=.027	p=.742
Tree crown size (m)	0.97	0.59	−0.02	0.66	1.00	0.25	−0.71	0.59
	p=.001	p=.160	p=.964	p=.109	p=.000	p=.585	p=.076	p=.161
Tree height (m)	0.92	0.86	0.29	0.82	0.89	0.30	−0.59	0.20
	p=.003	p=.014	p=.540	p=.025	p=.006	p=.551	p=.160	p=.671
Tree crown closure (%)	−0.32	−0.20	−0.31	−0.27	−0.24	−0.17	0.16	−0.07
	p=.494	p=.662	p=.506	p=.556	p=.601	p=.723	p=.729	p=.886
Tree stress index (1 to 5)	0.35	−0.01	−0.74	−0.14	0.47	0.86	−0.96	0.01
	p=.438	p=.984	p=.056	p=.767	p=.283	p=.013	p=.001	p=.979

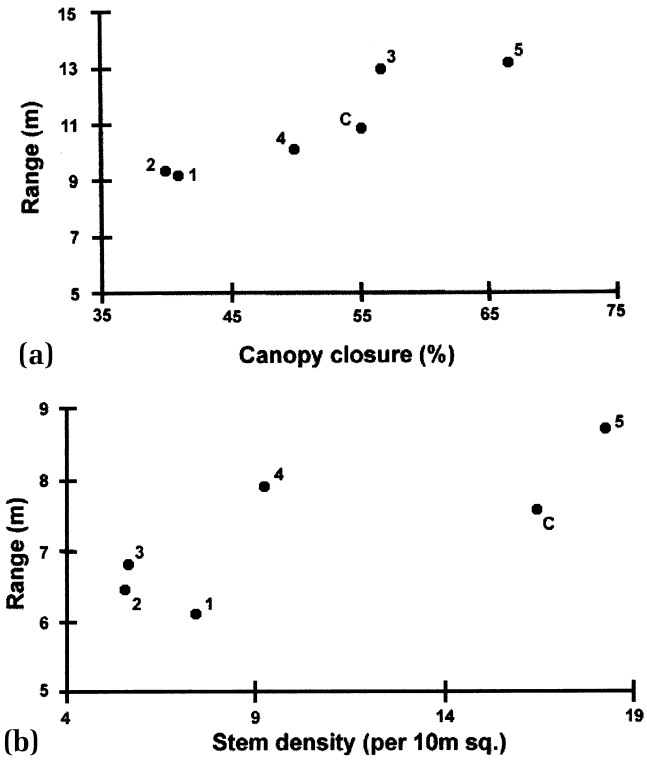

Figure 5. a) Range for transect semivariograms in the 1 m pixel image versus forest canopy closure (r=0.92); b) range for matrix semivariograms in the 1 m pixel image versus forest stem density (r=0.81).

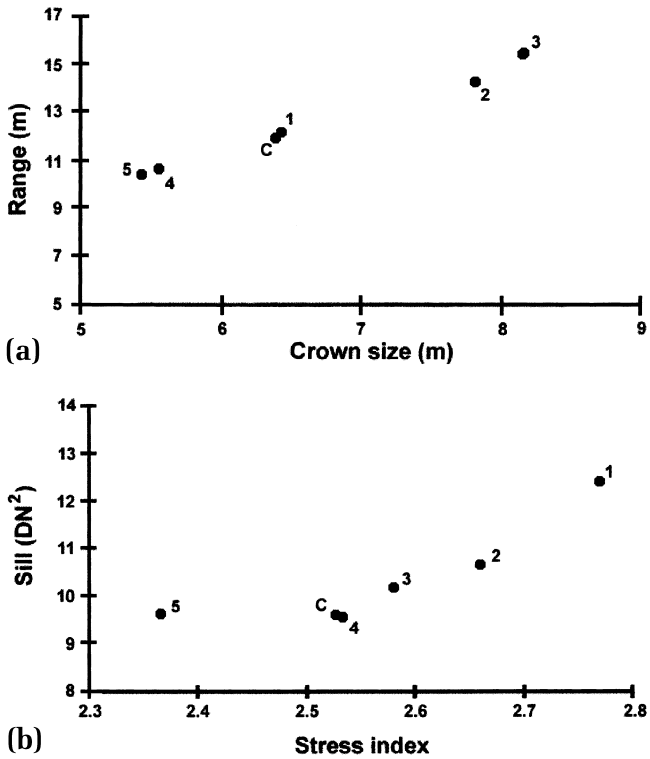

Figure 6. a) Range for matrix semivariograms in the 0.5 m pixel image versus tree crown size (r=1.0); b) sill for matrix semivariograms in the 0.5 m pixel image versus tree stress index (r=0.86).

the 0.5 m pixel matrix semivariogram. Range increases linearly with tree crown size in this highly significant relationship. Thus, the range of such a semivariogram may serve as an effective measure for automated derivation of the average crown size in stands over a region. This agrees with results of Cohen and Spies (1990). The 1 m semivariogram range was not sensitive to crown size for the trees of this study. The average width of trees in some plots was as low as 1.9–3 m (95% lower bounds for plots C, 4 and 5). The range of the semivariograms extracted from the canopy was not reached at such short lags as the support size was just less than or just larger than the object width. Consequently, the 1 m semivariograms cannot be used to detect such crown sizes, but they are sensitive to spatial variability over larger extents as described above for canopy closure.

Similarly to tree crown size, tree height is well associated with range values. Tree height in this forest is well correlated with crown size (r=0.85) so that its high correlation with the range in the 0.5 m pixel image using both the transect and matrix techniques was expected. The combined effect of height and size variations (e.g., as measured by the height-to-diameter ratio) produces variations in shadows and highlights that serve to delimit tree crowns. The sill of both the 0.5 m and 1 m transect semivariograms are also well related to tree height. The matrix semivariogram sill is not significantly related to this forest parameter, indicating that the transect technique is more sensitive to variation in tree height.

In analysis of the tree stress index, matrix semivariograms appear to be more suitable for determining the structural and textural information related to the visual stress symptoms included in the index. This measure represents the plot average of the overall health of individual trees and is a more integrated measure of forest damage than the other individual measures. The sill of the 0.5 m pixel matrix semivariograms is positively correlated to the stress index (Fig. 6b) which indicates that when the index is high (greater damage), the amount of spatial variability within crowns is higher, and this results in higher variability when sampling is conducted over the canopy. Figure 7 shows the relationship between the stress index and the range of the 1 m pixel matrix semivariograms. The two variables are negatively correlated, indicating that when the index is high, the range is small. This can again be explained by greater plot variability when variability within individual crowns is increased causing the range to be reached at a lesser distance than in a more homogeneous canopy. In a very open and nearly dead crown, with uniform background radiance, this negative relationship may not apply as the gray tone surface will already be homogeneous. However, in the

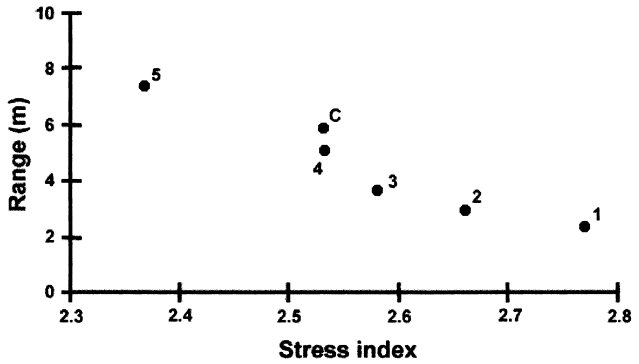

Figure 7. Range for matrix semivariograms in the 1 m pixel image versus tree stress index ($r=-0.96$).

high resolution imagery used in this research, and particularly in the high contrast near IR band, shadows from branches and spatial variability in understory vegetation generally produce a very heterogeneous gray tone surface. Any increase in foliage in the tree tends to increase the homogeneity of the gray tone surface and the negative relation with semivariance range still applies.

Among all the field measurements only the individual tree crown closure is not significantly correlated with any semivariogram parameters extracted over the forest canopy. The smallest pixel spacing analyzed at this scale, 0.5 m, is still too large to detect this individual tree measure. For typical crown sizes of 5–8 m, the individual openings in the crowns which contribute to the tree crown closure measurement are smaller than 0.5 m. Thus, subsequent analysis of 0.25 m pixel imagery (described after the next subsection) was expected to provide improved relations between tree crown closure and the semivariance parameters.

Analysis of the variation among semivariogram parameters extracted using the matrix technique in subplot quadrants within the 0.5 m pixel imagery did not reveal significant variability between quadrants except for the open area in plot 1 which was previously mentioned. There were also no significant correlations between the plot-level variance of the range and sill determined from the four quadrant values and the forest parameters.

Analysis of Semivariogram Shapes

In plotting the semivariograms of the canopy-scale analysis, several distinct shapes were commonly produced. A variety of semivariogram shapes were obtained from either the transect or matrix technique sampled over the forest canopy in the 1993 0.5 m and 1.0 m pixel imagery. The transect semivariograms show periodicity in the healthier plots away from the mine tailings. The matrix semivariograms do not show this characteristic but display smooth curves which result from averaging over several directions. Some of the 1 m pixel semivariograms extracted from transects in plot 1 (poorest overall health) are linear in shape. In linear semivariograms the range is not reached, indicating a moderate spatial continuity within the transect. This plot is not very dense, having a low canopy closure (Table 1) and a large opening about 15 m across its northwest corner. Thus, transects passing through more open plots or large openings in the canopy, where individual objects such as tree crowns do not exist, may display more linearly shaped semivariograms as the range is not reached within a reasonable sampling distance.

The nugget effect is consistently present in the 0.5 m pixel semivariograms. This means that the pixels do not show a perfect autocorrelation and indicates that there is a lot of random variation in the data at this resolution. While sampling over the canopy at this spatial resolution is sensitive to individual tree crown size, tree height, and the tree stress index, the high variability over of such small pixels can be considered to be mostly noise when the measure of interest is canopy closure within areas such as the 2500 m^2 sample areas of this study. The 1 m pixel semivariograms do not display a nugget effect, and they are more sensitive to the forest canopy closure and stem density. Thus, in canopy level sampling, semivariance analysis of 1 m pixel imagery appears better suited to the scale of measurement of forest canopy parameters while 0.5 m pixel spacing is better suited to modeling of individual tree measures.

Individual Tree Crown-Scale Image Semivariance Analysis

Since individual tree crown closure could not be modeled well in the previous canopy-scale semivariance analysis of 1993 0.5 m and 1 m pixel imagery, additional tests using matrix semivariograms extracted from within individual tree crowns in the 1995 0.25 m and 0.5 m pixel imagery were conducted. Table 3 shows that tree crown closure is strongly related to the range derived from the 0.25 m pixel image ($r=0.85$). The range increases with crown closure (similar to the findings for canopy closure in the canopy analysis of 1 m pixel data as given in Table 2 and Fig. 5a) because, for poplars such as these, in more dense crowns, the leaves are closer to each other and produce a more homogeneous gray tone surface in the imagery. This relationship is illustrated in Figure 8a. As a crown becomes stressed and opens up, the size of shadowed areas within the crown becomes larger and the leaves become more clustered. The range is therefore reached at a shorter lag, as shown in Figure 8a, where it varies from 0.7 m for open stressed crowns to 1.7 m for closed healthy crowns. These ranges are much smaller than all crown diameters, demonstrating the sensitivity of the semivariogram to within-crown variance. For very open and dying crowns, the same argument presented above for the stress index applies. That is, if the background signal in such a case was entirely uniform, addition of foliage would produce more heterogeneity and

Table 3. Correlation Coefficients (r) for the Relationships between Tree Crown Closure and the Semivariogram Parameters for 0.25 m and 0.5 m Pixel Images Derived from the Matrix Technique

	Range (0.25 m)	*Sill (0.25 m)*	*Range (0.5 m)*	*Sill (0.5 m)*
Crown closure	0.85	0.29	−0.16	0.06

relations with the range would be the inverse of that found here. However, the variability of the background and shadows in imagery with 0.25 m pixel spacing is very high, and an open tree crown produces a very heterogeneous gray tone surface. Thus, dead or nearly dead trees would not be expected to produce model deviations from the positive relation with the range that was found.

None of the other semivariance parameters, at either image resolution, provided significant relations with tree crown closure. Sampling within individual crowns in the 1995 0.5 m pixel data did not improve the relations with tree crown closure over those derived from canopy sampling in the 1993 0.5 m pixel data (Table 2). The range of the 1995 0.5 m pixel image does not show any correlation with tree crown closure. This is illustrated in Figure 8b, where 14 points out of 20 are located at the 3.5 m range. This distance represents the range limit above which not enough pairs of pixels are available to calculate a significant estimate of the semivariance. These semivariograms never reach the range of influence and display a linear function. The support size is too large to detect the variability caused by shadows and highlights within single tree crowns, confirming that a pixel spacing smaller than 0.5 m is needed to analyze the structure of the individual tree crowns.

Figure 8. a) Range for matrix semivariograms in the 0.25 m pixel image versus tree crown closure (r=0.85); b) range for matrix semivariograms in the 0.5 m pixel image versus tree crown closure (r=−0.16). Note that fewer points than were generated are displayed in the graph since some fall at the same positions.

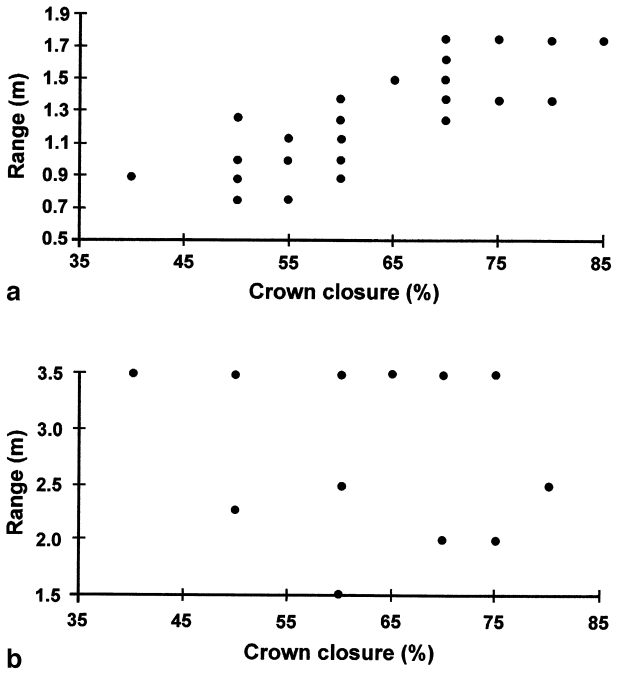

Relations of Forest Parameters with Mean Gray Level and First-Order Texture

Analysis of relations of the forest parameters with mean gray level and a simple first-order texture measure was conducted for comparison to the results derived from the preceding semivariance analysis. Results show that the mean gray level of forest canopy or individual tree samples is not highly correlated with any of the forest parameters for any of the pixel sizes tested. Correlation coefficients ranged from 0.01 to 0.58, none being statistically significant. As a simple first-order texture measure, the standard deviation was also evaluated. Correlation coefficients were slightly greater, ranging from 0.03 to 0.81, the latter being against the health index in the 1 m pixel data and the only statistically significant relation at the 0.05 level. Thus, the semivariance analysis has identified several significant relationships between image and forest parameters which are not evident in single band raw spectral data nor in simple first-order image texture.

CONCLUSIONS

This study has demonstrated the usefulness of semivariogram shape and statistical analysis in discrimination of forest structural damage variations at the KamKotia mine site. Matrix (omnidirectional) semivariogram parameters were well correlated with a visual tree stress index and transect semivariograms were better correlated with tree height, but both were sensitive to tree crown size and canopy closure. The two techniques are complementary if all the forest measurements are considered. Otherwise, the appropriate technique can be selected for the forest parameter to be evaluated.

In sampling over the forest canopy, the 0.5 m pixel semivariograms uniquely captured information about the tree crown size while the 1 m pixel semivariograms were better correlated with forest canopy closure and stem density. This shows that determination of the appropriate object size for a given support size is critical. Pixels of 1 m are not sensitive to the tree sizes of this study but are quite sensitive to the spatial variation of trees and gaps over a larger spatial extent as measured by canopy closure. Both spatial resolutions were sensitive to tree

health and average tree height. The 0.5 m pixel semivariograms included some random variation (nugget effect) that was not present in the 1 m pixel semivariograms. This suggests that the 1 m pixel semivariograms are more appropriate to canopy level analysis and are better for interpretation of the shape of the semivariograms. The 1 m pixel semivariograms were smoother, and the curves and peaks were attenuated while the 0.5 m pixel semivariograms had a nugget which flattened the function curve and masked much of its structural information.

Individual tree crown closure was not significantly correlated with any of the 0.5 m and 1 m pixel semivariogram parameters extracted by canopy sampling. For example, in 70% of the cases, the 0.5 m pixel image semivariograms displayed a linear shape that indicates that the range was not reached and that this resolution is too coarse to depict tree crown structural information. It is an aggregate measure of much smaller physical elements than the other forest parameters. Capture of this information in semivariograms requires finer spatial resolution and image samples collected from individual tree crowns only. This structural information of tree crowns was modeled well using images of 0.25 m pixel spacing. The range was found to increase with tree crown closure since a more homogeneous gray tone surface produces a larger range. The 0.25 m pixel image semivariograms displayed a spherical shape that shows that the range was reached at this spatial resolution. These results may have strong implications in analysis of forest damage where individual trees vary significantly in damage level.

The relations between semivariance parameters and forest and tree structural measures discovered in this study should be interpreted with caution as they were generated from a very homogeneous forest stand of essentially one overstory species and small ranges of forest structural parameters (although some plot pairs showed statistically significant differences for some variables). There is a need for more research under a variety of composition, structure, and imaging conditions. We are currently pursuing all of these aspects in ongoing research to develop a quantitative stress index based on image spectral, textural, and structural characteristics. In addition, besides results previous listed, progress has been made on integration of image spectral information and other texture measures (Olthof and King, 1997) and image structural information using the proportion of shadow in the canopy (Seed and King, 1997). The combination of these three fundamental image components in the stress index should improve its power for detection and quantification of the various kinds of stress symptoms evident at such mine sites. The methods and results of this study may also provide benefit in other fields such as ecological modeling, forest vegetation management, and climate studies where forest structure information is required at a variety of scales.

This research was supported by the Natural Sciences and Engineering Research Council (NSERC) of Canada to D. King, the Ontario Ministry of Natural Resources (Timmins), and the Ontario Provincial Remote Sensing Office.

REFERENCES

Bowers, W. W., Franklin, S. E., Hudak, J., and McDermid, G. J. (1994), Forest structural damage analysis using image semivariance. *Can. J. Remote Sens.* 20:28–36.

Cohen, W. B., and Spies, T. A. (1990), Semivariograms of digital imagery for analysis of conifer canopy structure. *Remote Sens. Environ.* 34:167–178.

Coops, N. C., and Catling, P. C. (1997), Predicting the complexity of habitat in forests from airborne videography for wildlife management. *Int. J. Remote Sens.* 18:2677–2682.

Curran, P. J. (1988), The semivariogram in remote sensing: an introduction. *Remote Sens. Environ.* 24:493–507.

Curtiss, B., and Maecher, A. G. (1991), Changes in forest canopy reflectance associated with chronic exposure to high concentrations of soil trace metals. In *Proc. 8th Thematic Conference on Geologic Remote Sensing*, (ERIM), Denver, CO, 29 April–2 May, pp. 337–347.

Englund, E., and Sparks, A. (1991), *GEOEAS User's Guide*, EPA 6008-91008, U.S. Environmental Protection Agency, Las Vegas, NV.

Kelley, B. C., and Tuovinien, O. H. (1988), Microbiological oxidation of minerals in mine tailings. In *Chemistry and Biology of Solid Waste* (W. Salomons and U. Forstner, Eds.), Springer-Verlag, New York, pp. 33–53.

King, D. J. (1995a), Airborne multispectral digital camera and video sensors: a critical review of system designs and applications. *Can. J. Remote Sens. (Special Issue on Aerial Optical Remote Sensing)* 21:245–273.

King, D. J. (1995b), Development of an airborne multispectral digital frame camera sensor. In *Proc. 15th Biennial Workshop on Color Photography and Videography in Resource Assessment*, Am. Soc. Photogramm. and Remote Sens., Terre Haute, IN, 2–3 May, pp. 13–22.

Lévesque, J., and King, D. J. (1993), Évaluation des dommages forestiers causés par le drainage acide provenant des mines à l'aide d'une caméra numérisante multispectrale: aperçu du projet et résultats préliminaires. In *Proc. 16th Canadian Symposium on Remote Sensing*, Can Remote Sens. Soc., Sherbrooke, Québec, 8–10 June, pp. 657–662.

Li-COR Inc. (1990), *LAI-2000 Plant Canopy Analyzer: Technical Information Manual*, LI-COR Inc., Lincoln, NE.

McIlveen, W. D., McLaughlin, D. L., and Arnup, R. W. (1989), A survey to document the decline status of the sugar maple forest of Ontario: 1986, Ontario Ministry of Environment Publication, ISBN 0-7729-6253-7, 22 pp.

Murtha, P. A. (1978), Remote sensing and vegetation damage: a theory for detection and assessment. *Photogramm. Eng. Remote Sens.* 44:1147–1158.

Olthof, I., and King, D. J. (1998), Determination of soil property and forest structure relations with airborne digital camera image spectral and spatial information. In *Proc. of the 20th Canadian Symposium on Remote Sensing*, Calgary, Alberta, 10–13 May, pp. 103–106.

Olthof, I., and King, D. J. (1997), Evaluation of textural information in airborne CIR digital camera imagery for estimation of forest stand leaf area index. In *Proc. 1st North American Symposium on Small Format Aerial Photography*, Am. Soc. for Photogramm. and Remote Sens., Cloquet, MN, 14–17 October, pp. 154–164.

Pannatier, Y. (1994), Variowin 2.1, Institute of Mineralogy BFSH2, University of Lausanne, Switzerland.

Peterson, E. B., and Peterson, N. M. (1992), Ecology, management, and use of aspen and balsam poplar in the prairie provinces, Forestry Canada Special Report 1, Northwest Region, Northern Forestry Centre, Edmonton, Alberta, 252 pp.

Seed, E. D., and King, D. J. (1997), Determination of mixed boreal forest stand biophysical structure using large scale airborne digital camera imagery. In *Proc. GER '97/19th Canadian Symposium on Remote Sensing*, Natural Resources Canada, 24–30 May, Ottawa, Ontario, CD-ROM, article #75, 8 pp.

St-Onge, B. A., and Cavayas, F. (1995), Estimating forest stand structure from high resolution imagery using the directional variogram. *Int. J. Remote Sens.* 16:1999–2021.

Walsworth, N., and King, D. J. (1999), Image modeling of forest changes associated with acid mine drainage. *Comput. Geosci.* (in press).

Woodcock, C. E., Strahler, A. H., and Jupp, D. L. B. (1988a), The use of variograms in remote sensing: I. Scene models and simulated images. *Remote Sens. Environ.* 25:323–348.

Woodcock, C. E., Strahler, A. H., and Jupp, D. L. B. (1988b), The use of variograms in remote sensing: II. Real digital images. *Remote Sens. Environ.* 25:349–379.

Wulder, M. A., Lavigne, M. B., LeDrew, E. F., and Franklin, S. E. (1997), Comparison of texture algorithms in the statistical estimation of LAI: first-order, second-order, and semivariance moment texture (SMT). In *Proc. GER '97/19th Canadian Symposium on Remote Sensing*, Natural Resources Canada, 24–30 May, Ottawa, Ontario, CD-ROM.

Yuan, X. Y., King, D. J., and Vlcek, J. (1991), Sugar maple decline assessment based on spectral and textural analysis of multispectral aerial videography. *Remote Sens. Environ.* 37:47–54.